GEOPHYSICAL RESEARCH LETTERS, VOL. 36, L18610, doi:10.1029/2009GL040055, 2009

Evidence of sediment resuspension by island trapped waves

Antoni Jordi,[1] Gotzon Basterretxea,[1] and Dong-Ping Wang[2]

Received 17 July 2009; revised 19 August 2009; accepted 31 August 2009; published 29 September 2009.

[1] Six months of current and acoustic backscatter data from an acoustic Doppler current profiler (ADCP) moored in the shelf off Mallorca (Balearic Islands, Mediterranean Sea) were analyzed. The presence of island trapped waves (ITWs) was determined by correspondence of energetic subinertial peaks in the alongshore current spectra with theoretical wave modes. Although currents in this area averaged 0.06 m/s and rarely exceeded 0.5 m/s, an intense episode with currents larger than 1 m/s was observed between March 8 and 11, 2007. Our analysis demonstrates that ITWs generated by local wind forcing were responsible for such currents, causing significant sediment resuspension on those days. It is suggested that even moderate wind pulses can induce important resuspension along the shelf by generating ITWs. This could be an overlooked mechanism of coupling between atmospheric and shelf circulation with significant implications for sediment dynamics and biogeochemical cycles. **Citation:** Jordi, A., G. Basterretxea, and D.-P. Wang (2009), Evidence of sediment resuspension by island trapped waves, *Geophys. Res. Lett.*, *36*, L18610, doi:10.1029/2009GL040055.

1. Introduction

[2] Coastal trapped waves (CTWs) are known to be an important component of the circulation over the continental margins on timescales greater than the inertial period, that they often play a role in the response of the ocean to atmospheric weather changes. CTWs are mainly generated by surface wind stress and, through their propagation with the coast on the right (left) in the Northern (Southern) Hemisphere, spread the ocean's response over considerable distances along the shelf. A review of observational and theoretical studies of CTWs on continental margins was given by *Huthnance et al.* [1986] and *Brink* [1991]. A special case of CTWs occurs around islands because waves with an integer number of wavelengths, or continuous phase, around the island reinforce themselves [*Mysak*, 1967; *Longuet-Higgins*, 1970]. As a result of this resonance, ITWs are associated with a discrete spectrum of wavelengths that approach the azimuthal phase continuity. The theoretical context for linear ITWs around a circular island with stratification and bottom relief was provided by *Brink* [1999].

[3] The present work is part of a wider study aimed at understanding the circulation patterns in southern Mallorca. In this Mediterranean region, currents are weak and largely uncoupled from open-ocean circulation. Atmospherically forced ITWs are found to be a major source of the observed current fluctuations. Although there is observational evidence of ITWs around islands in other regions [e.g., *Wunsch*, 1972; *Hogg*, 1980], to our knowledge, no previous study has reported of their role on sediment resuspension. In the absence of significant tides and the generally weak coastal currents and swells, sediment resuspension in the Mediterranean is restricted to episodic energetic events. *Guillén et al.* [2002] and *Puig et al.* [2007] have studied the influence of storm waves on sediment transport. Also, long waves, such as seiches, are known to control episodic sediment resuspension in semi-enclosed areas [*Jordi et al.*, 2008]. Yet, other mechanisms contributing to sediment dynamics in microtidal areas, such as ITWs, have been largely overlooked.

[4] Up to now, trapped waves in the Mediterranean only have been identified along the continental margins of the Gulf of Lions and Catalan Sea [*Jordi et al.*, 2005], but they may be also important in other areas. In this study, we present evidence of the importance of ITWs for shelf dynamics. We identify the presence of ITWs around Mallorca by correspondence of energetic peaks in coastal current spectra with theoretical wave modes. We also report the key role of ITWs on resuspension events in the Mallorca shelf based on data obtained from an acoustic Doppler current profiler (ADCP).

2. Data and Methods

2.1. Field Observations

[5] A bottom mounted ADCP (1 MHz Nortek Aquadopp) was deployed from February 27 to August 31, 2007 in the Mallorca shelf at a depth of 25 m (Figure 1). Vertical profiles of current velocities and acoustic backscatters (or echo intensities) were measured every 30 min at 4 m depth intervals with the first level 3 m above the bottom (3 mab). The echo intensity was used as an estimation of suspended particle concentration in the water column, because there is a good correlation between the acoustic signal and the suspended particle concentration [e.g., *Thorne and Hanes*, 2002]. The scattering range for a 1 MHz ADCP is about 50–1500 μm in size. Since the sea floor around the ADCP location is mostly composed of sandy sediments with an average particle size of 295 ± 25 μm [*Intecsa*, 1991], the ADCP is capable of providing measurements of suspended sediments. Biological particles, such as zooplankton and large phytoplankton, are also in the scattering range of the ADCP and can affect ADCP measurements.

[6] Additionally, wind velocity data were obtained from a nearby permanent station located in Mallorca Airport by the Spanish Meteorological Service (AEMET). The spectral contents for currents and winds were estimated using a Hamming window of 20 days (960 points) with half

[1] IMEDEA (UIB-CSIC), Institut Mediterrani d'Estudis Avançats, Illes Balears, Spain.
[2] School of Marine and Atmospheric Sciences, Stony Brook University, Stony Brook, New York, USA.

0094-8276/09/2009GL040055

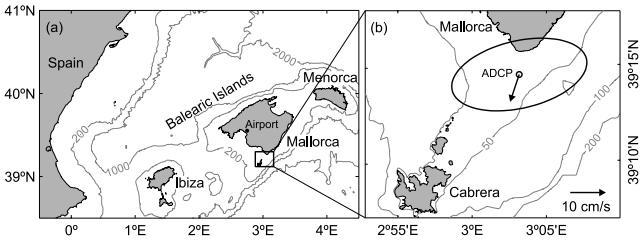

Figure 1. Study area: (a) bathymetry around the Balearic Islands (Mediterranean Sea), and (b) bathymetry in the southern shelf of Mallorca showing the ADCP location (open circle), the mean bottom current (arrow) and variance (ellipse).

window overlapping. Wave estimations from the Spanish National Harbor Service (*Puertos del Estado*) were obtained near the ADCP location. Bottom wave orbital velocities were computed by linear wave theory and bottom shear stress due to the combined motion of waves and currents was estimated using the analytical theory of *Grant and Madsen* [1986].

2.2. ITWs Theory

[7] Considering motions with frequencies smaller than the inertial frequency f confined to the vicinity of a circular isolated island with the coast at radius $r = r_0$ and the bottom depth $h(r)$ increasing monotonically with radius until reaching a constant depth, the linear equations of motion for a stratified ocean can be solved by expanding the perturbation pressure p as free ITW modal structures F^{nm} [*Brink*, 1999]

$$p(r,\theta,z,t) = F^{nm}(r,z)\exp[i(\omega^{nm}t + m\theta)] \tag{1}$$

where r, θ and z are the radial, azimuthal and vertical coordinates, t is time, n and m are the azimuthal and radial mode number, and ω^{nm} represents the free wave frequencies. The free ITW modal structures are solutions to the following equation

$$\left[f^2 - (\omega^{nm})^2\right]\left(\frac{F_z^{nm}}{N^2}\right)_z + \frac{1}{r}\left(rF_r^{nm}\right)_r - \frac{m^2}{r^2}F^{nm} = 0 \tag{2a}$$

subject to the boundary conditions

$$\left[f^2 - (\omega^{nm})^2\right]\frac{F_z^{nm}}{N^2} + h_r\left(F_r^{nm} + \frac{mf}{r}\frac{F^{nm}}{\omega^{nm}}\right) = 0 \quad \text{at} \quad z = -h(r) \tag{2b}$$

$$F_z^{nm} = 0 \quad \text{at} \quad z = 0 \tag{2c}$$

$$F_r^{nm} + \left(\frac{mf}{r\omega^{nm}}\right)F^{nm} = 0 \quad \text{at} \quad r = r_0 \tag{2d}$$

$$F_n \to 0 \quad \text{at} \quad r \to \infty \tag{2e}$$

where N is the buoyancy frequency, and subscripts r and z represent partial differentiations. The boundary conditions represent no flow through the bottom (equation (2b)), a rigid lid (equation (2c)), no flow through the coast (equation (2d)), and coastal boundedness at large radius (equation (2e)).

3. Results

3.1. General Conditions

[8] Winds and bottom currents (3 mab) were usually small during the study period (Figure 2). Winds greater than 8 m/s were registered 10 times and currents rarely exceeded 0.5 m/s during the study period, although intense currents of about 1 m/s were registered on March 8 and 11 coincident with episodes of enhanced wind. The mean current was also small (0.06 m/s) and directed to the south following the bottom topography (Figure 1). The principal axis of the variance ellipse was almost perpendicular to the mean current. We consider that the direction of the principal axis corresponds to the alongshore direction. The currents were essentially homogeneous through the water column; correlation coefficients between the bottom currents and currents at other depth levels were greater than 0.8 for both components (not shown). Therefore we focus our analysis on the bottom currents, although results are similar for currents at other depths.

3.2. Identification of ITWs

[9] The alongshore and cross-shore current spectral contents are shown in Figure 3a. The alongshore currents were more energetic and major peaks were observed at a period of 56.9 h, at diurnal/semidiurnal periods (24.1 and 12.4 h) and at inertial period (19.3 h). To find out whether ITWs are responsible for those peaks, the governing equation (2) were solved numerically using resonance iteration on a vertically stretched finite difference grid having 67 radial grid points and 30 grid points in the vertical. Topography was calculated as an average of the Mallorca's major and minor axes, with the water depth set to 10 m at the coast (r_0 = 30.8 km). A stratification profile around Mallorca was horizontally averaged from MedAtlas database (http://www.ifremer.fr/medar/) for the period when the ADCP was deployed. Results show that the periods associated with the first two radial (n = 1, 2) and first azimuthal (m = 1) ITW free modes are 23.8 and 55.8 h, respectively. Although errors associated with computing the free modes can arise from a number of sources and can be large [*Brink*, 1999], the agreement between this theoretical result and observed periods is quite good, suggesting that spectral peaks are ITW modes. The period of the gravest mode (n, m = 1) is in the vicinity of the diurnal tidal period. However, tidal signals were estimated by an iteratively reweighted least squares calculation of harmonic analysis [*Pawlowicz et al.*, 2002; *Leffler and*

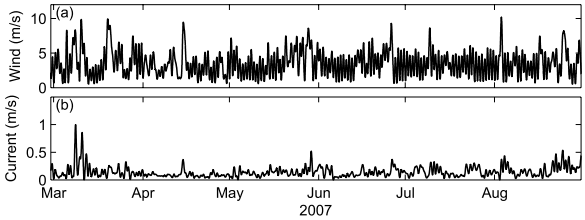

Figure 2. General conditions during the study period: time series of (a) low passed wind speed (m/s), and (b) low passed bottom current intensity (m/s).

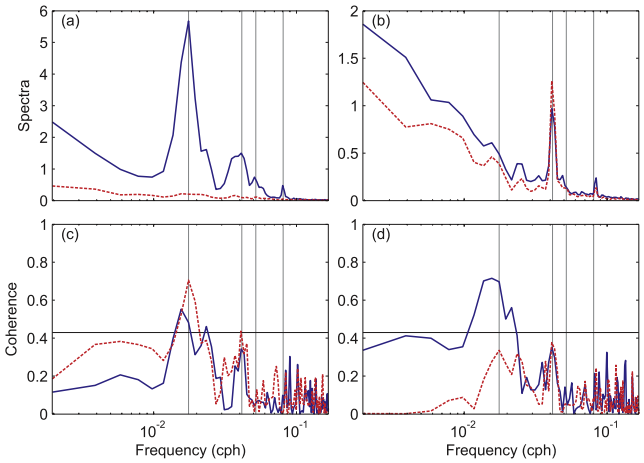

Figure 3. Spectral analysis: (a) alongshore (blue line) and cross-shore (dashed red line) bottom current spectral density (m^2/s), (b) east (blue line) and north (dashed red line) wind components spectral density (m^2/s), (c) spectral coherence between alongshore bottom current and east (blue line) and north (dashed red line) wind components, and (d) clockwise (blue line) and counterclockwise (dashed red line) spectral coherence between alongshore bottom current and wind. Vertical grey lines are periods of 56.9, 24.1, 19.3, and 12.4 h. Horizontal black lines represent the 95% confidence limit for coherence.

Jay, 2009] and the diurnal tidal currents were less than 0.03 m/s. The spectral peak at 24.1 h was slightly reduced when the tidal signal was removed (not shown). Further evidence for an ITW mode in this period will be given next.

3.3. Generation of ITWs

[10] We study the possibility that local wind generates the ITWs. The east and north wind component spectral contents showed peaks at the diurnal and semi-diurnal frequencies (Figure 3b). However, the alongshore current and each wind component were significantly coherent (at 95% level or more) around the periods of 56.9 h and 24.1 h (Figure 3c), indicating that local wind generated the ITWs. The spectral coherence was estimated using each wind component as separate scalar time series. This method can be extended for getting rotary components using both wind components as a complex time series [*Gonella*, 1972; *Mooers*, 1973]. Since the ITWs travel clockwise around the island in the Northern Hemisphere, the clockwise rotation of the wind in time is expected to be more effective to generate this ITW mode. Figure 3d shows the rotary coherence between alongshore current and wind with a significant peak around 56.9 h for the clockwise coherence. This is in agreement with the results of *Merrifield et al.* [2002] at the Hawaiian Islands.

3.4. Role of ITWs

[11] To analyze the role of ITWs on sediment resuspension, we focus on the period from March 4 to 15 when intense currents of more than 1 m/s were found associated with episodes of northward wind intensification (Figure 4). To elucidate the contribution of the first two radial (n = 1, 2) and first azimuthal (m = 1) modes, bottom alongshore currents were band-pass filtered centered on the 56.9 and 24.1 h periods. These two modes increased on March 5 as a consequence of a first episode of wind enhancement of a diurnal period. A second intensification of both modes occurred associated with the wind enhancement and clockwise rotation on March 8. In addition, both modes were almost in phase, contributing to the observed intense current. Despite that winds notably weakened on March 9, both modes slightly increased from March 8 to 11 which is indicative of ITW resonance. On March 11, both modes were again in phase and a second current peak occurred.

[12] Two major peaks of echo intensity were correlated with the two events of bottom alongshore currents larger than 1 m/s (Figure 4d), suggesting that the peaks correspond to sediment resuspension. Waves can also be responsible for the sediment resuspension. However, the ADCP location was protected from northern seas and significant wave height in the area was below 2.5 m (Figure 4e). The bottom wave orbital velocities were about 0.4 m/s during the two wind enhancements, much smaller than the bottom currents induced by the ITWs. Another possibility is that these peaks were caused by sediments transported from shallower areas. However, most of the bottom between 5 and 20 m is composed by seagrass meadows and it is unlikely that significant amounts of sediment could be supplied from these areas. Furthermore, the bottom shear stress during the two peaks was much greater than 0.35 N/m^2 (Figure 4b), which theoretically is sufficient to stir up fine sand sediments.

[13] In addition to these two peaks, sharper peaks not correlated with strong currents appeared generally at dusk, which is attributed to vertically migrating zooplankton. The correlation between ADCP acoustic signal and zooplankton abundance is well known [*Flagg and Smith*, 1989]. *Pinot and Jansá* [2001] used data from an ADCP in the nearby Ibiza Channel to identify zooplankton diel migration, ascending at dusk and descending at dawn. The sharper peaks at

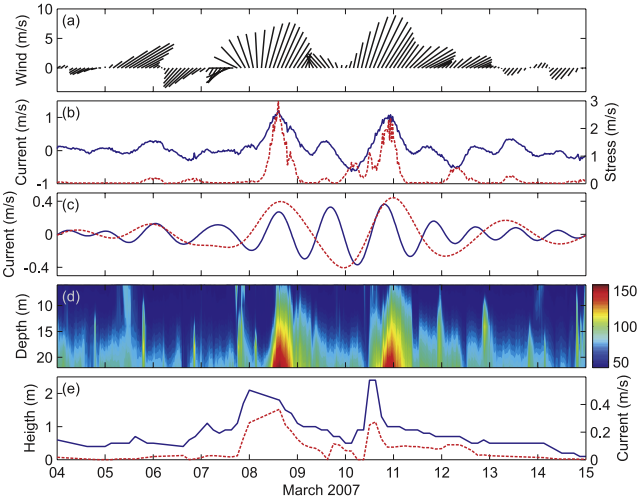

Figure 4. Resuspension event associated with ITWs: time series of (a) low passed wind (m/s), (b) alongshore bottom current (m/s, positive values toward 9.1° southwest, blue line) and total shear stress (N/m^2, dashed red line), (c) band passed bottom alongshore currents (m/s) for the first (n = 1 and m = 1, blue line) and second (n = 2 and m = 1, dashed red line) radial modes, (d) ADCP echo intensities (dB), and (e) significant wave height (m, blue line) and bottom orbital current (m/s, dashed red line).

dusk agree with the zooplankton ascension, although few peaks also were observed at dawn.

4. Conclusion

[14] The analysis of ADCP data from southern Mallorca demonstrates the existence of island trapped waves (ITWs). A reasonable agreement between observed spectral periods and theoretical wave modes was obtained. ITWs were generated by the local wind and, particularly, its clockwise rotation. Remarkably intense currents for this region (>1 m/s) were induced by an ITW response on March 8 and 11, 2007. An increased concentration of particulates in the water column was associated with these ITWs, representing the first evidence of sediment resuspension by ITWs. These results suggest that in microtidal areas ITWs can exert an important influence on ocean-margin circulation, mixing, sediment dynamics and biogeochemistry.

[15] It is interesting that the dominant ITW signal is at the second radial mode (n = 2) rather than the first (Figure 3). Since the two wind bursts during the resuspension event are a little over 2 days apart, the spectral analysis could presumably be dominated by this event which is close to the period of the second mode (56.9 h). However, the alongshore current spectrum computed without the resuspension event still shows a greater second mode. Our explanation is that the diurnal wind is associated with the sea breeze, which has a limited offshore scale and the wind tends to blow across shore. In contrast, typical weather systems have spatial scales larger than Mallorca and can force the second mode. Also, the sea breeze does not rotate with time, which is important for the generation of ITWs.

[16] We are aware that assessing the overall relevance of this process requires knowledge on its recurrence. In the 6 months of data examined, winds were greater than 8 m/s about 10 times and this was the unique ITW event with currents about 1 m/s. However, winds that generated this ITW event were not exceptionally extreme and ITWs were reinforced by the clockwise rotation of winds. On the other hand, storms and extreme winds in the Mediterranean are more frequent in winter than in summer when the ADCP was deployed. A more comprehensive study of ITWs in this region to elucidate this issue is needed.

[17] **Acknowledgments.** This work was partly supported by the Ministerio de Medio Ambiente project TALACA (38/2006). A. Jordi's work was supported by a JAE-Doc grant from CSIC. We are grateful to AEMET and *Puertos del Estado* for providing wind and wave data.

References

Brink, K. H. (1991), Coastal-trapped waves and wind-driven currents over the continental-shelf, *Annu. Rev. Fluid Mech.*, *23*, 389–412, doi:10.1146/annurev.fl.23.010191.002133.

Brink, K. H. (1999), Island-trapped waves, with application to observations off Bermuda, *Dyn. Atmos. Oceans*, *29*, 93–118, doi:10.1016/S0377-0265(99)00003-2.

Flagg, C. N., and S. L. Smith (1989), On the use of the acoustic Doppler current profiler to measure zooplankton abundance, *Deep Sea Res., Part A*, *36*, 455–474, doi:10.1016/0198-0149(89)90047-2.

Gonella, J. (1972), Rotary-component method for analyzing meteorological and oceanographic vector time series, *Deep Sea Res.*, *19*, 833–846.

Grant, W. D., and O. S. Madsen (1986), The continental-shelf bottom boundary-layer, *Annu. Rev. Fluid Mech.*, *18*, 265–305, doi:10.1146/annurev.fl.18.010186.001405.

Guillén, J., J. A. Jiménez, A. Palanques, V. Gracía, P. Puig, and A. Sánchez-Arcilla (2002), Sediment resuspension across a microtidal, low-energy inner shelf, *Cont. Shelf Res.*, *22*, 305–325, doi:10.1016/S0278-4343(01)00059-0.

Hogg, N. G. (1980), Observations of internal Kelvin waves trapped round Bermuda, *J. Phys. Oceanogr.*, *10*, 1353–1376, doi:10.1175/1520-0485(1980)010<1353:OOIKWT>2.0.CO;2.

Huthnance, J. M., L. A. Mysak, and D.-P. Wang (1986), Coastal trapped waves, in *Baroclinic Processes on the Continental Shelves*, edited by C. N. K. Mooers, pp. 1–18, AGU, Washington, D. C.

Intecsa (1991), *Estudio Geofísico Marino Entre Cabo Freu y Cabo Salinas (Mallorca)*, Minist. de Obras Publicas y Transp., Madrid.

Jordi, A., A. Orfila, G. Basterretxea, and J. Tintoré (2005), Coastal trapped waves in the northwestern Mediterranean, *Cont. Shelf Res.*, *25*, 185–196, doi:10.1016/j.csr.2004.09.012.

Jordi, A., G. Basterretxea, B. Casas, S. Anglès, and E. Garcés (2008), Seiche-forced resuspension events in a Mediterranean harbour, *Cont. Shelf Res.*, *28*, 505–515, doi:10.1016/j.csr.2007.10.009.

Leffler, K. E., and D. A. Jay (2009), Enhancing tidal harmonic analysis: Robust (hybrid L-1/L-2) solutions, *Cont. Shelf Res.*, *29*, 78–88, doi:10.1016/j.csr.2008.04.011.

Longuet-Higgins, M. S. (1970), Steady currents induced by oscillations round islands, *J. Fluid Mech.*, *42*, 701–720, doi:10.1017/S0022112070001568.

Merrifield, M. A., L. Yang, and D. S. Luther (2002), Numerical simulations of a storm-generated island-trapped wave event at the Hawaiian Islands, *J. Geophys. Res.*, *107*(C10), 3169, doi:10.1029/2001JC001134.

Mooers, C. N. K. (1973), A technique for cross spectrum analysis of pairs of complex-valued time series, with emphasis on properties of polarized components and rotational invariants, *Deep Sea Res.*, *20*, 1129–1141.

Mysak, L. A. (1967), On the theory of continental shelf waves, *J. Mar. Res.*, *25*, 205–227.

Pawlowicz, R., B. Beardsley, and S. Lentz (2002), Classical tidal harmonic analysis including error estimates in MATLAB using T-TIDE, *Comput. Geosci.*, *28*, 929–937, doi:10.1016/S0098-3004(02)00013-4.

Pinot, J. M., and J. Jansá (2001), Time variability of acoustic backscatter from zooplankton in the Ibiza Channel (western Mediterranean), *Deep Sea Res., Part I*, *48*, 1651–1670, doi:10.1016/S0967-0637(00)00095-9.

Puig, P., A. S. Ogston, J. Guillén, A. M. V. Fain, and A. Palanques (2007), Sediment transport processes from the topset to the foreset of a crenulated clinoform (Adriatic Sea), *Cont. Shelf Res.*, *27*, 452–474, doi:10.1016/j.csr.2006.11.005.

Thorne, P. D., and D. M. Hanes (2002), A review of acoustic measurement of small-scale sediment processes, *Cont. Shelf Res.*, *22*, 603–632, doi:10.1016/S0278-4343(01)00101-7.

Wunsch, C. (1972), Spectrum from 2 years to 2 minutes of temperature fluctuations in main thermocline at Bermuda, *Deep Sea Res.*, *19*, 577–593.

G. Basterretxea and A. Jordi, IMEDEA (UIB-CSIC), Institut Mediterrani d'Estudis Avançats, Miquel Marqués 21, Esporles, E-07190 Illes Balears, Spain. (toni@imedea.uib-csic.es)

D.-P. Wang, School of Marine and Atmospheric Sciences, Stony Brook University, Stony Brook, NY 11794, USA.